ORGANOMETALLICS

Article

pubs.acs.org/Organometallics

Living Ring-Opening Metathesis–Polymerization Synthesis and Redox-Sensing Properties of Norbornene Polymers and Copolymers Containing Ferrocenyl and Tetraethylene Glycol Groups

Haibin Gu,[†,§] Amalia Rapakousiou,[†] Patricia Castel,[†] Nicolas Guidolin,[‡] Nöel Pinaud,[†] Jaime Ruiz,[†] and Didier Astruc*[,†]

[†]ISM, UMR CNRS No. 5255, University of Bordeaux, 33405 Talence Cedex, France

[‡]LCPO, UMR CNRS No. 5629, University of Bordeaux, 33607 Pessac Cedex, France

Supporting Information

ABSTRACT: The controlled synthesis of monodisperse, redox-active metallopolymers and their redox properties and functions, including robust electrode derivatization and sensing, remains a challenge. Here a series of polynorbornene homopolymers and block copolymers containing side-chain amidoferrocenyl groups and tetraethylene glycol linkers were prepared via living ring-opening metathesis polymerization initiated by Grubbs' third-generation catalyst (**1**). Their molecular weights were determined using MALDI-TOF mass spectra, size exclusion chromatography (SEC), end-group analysis, and the empirical Bard–Anson electrochemical equation. All polymerizations followed a living and controlled manner, and the number of amidoferrocenyl units varied from 5 to 332. These homopolymers and block copolymers were successfully used to prepare modified Pt electrodes that showed excellent stability. The modified Pt electrodes show excellent qualitative sensing of ATP^{2-} anions, in particular those prepared with the block copolymers. The quantitative recognition and titration of $[n\text{-}Bu_4N]_2[ATP]$ was carried out using the CH_2Cl_2 solution of the homopolymers, showing that two amidoferrocenyl groups of the homopolymers interacted with each ATP^{2-} molecule. This stoichiometry led us to propose the H-bonding modes in the supramolecular polymeric network.

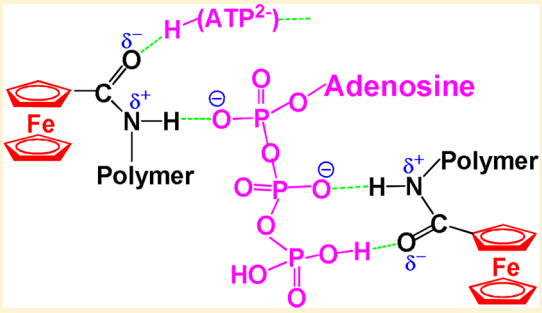

1. INTRODUCTION

The past several decades have witnessed the rapid development of metallocene-containing macromolecules, especially with ferrocenyl groups,[1−23] owing to their multielectron redox properties and wide applications such as catalysts,[24] biosensors,[25] virus-like receptors,[26] models of molecular batteries,[27] colorimetric sensors,[28] etc. Among the polymers, there are two major classes of materials: (i) main chain ferrocene containing polymers in which the ferrocenyl group is an integral part of the polymer backbone[29] and (ii) side chain ferrocene containing polymers in which the ferrocenyl moiety is a pendant group.[12,13] For the side chain ferrocene containing polymers, early studies focused mainly on vinylferrocene and ferrocene containing acrylate and methacrylate that were polymerized by conventional techniques such as free radical, cationic, and anionic polymerization. The polymers that were prepared using these methods often had low molecular weight (<10000) and lacked control of the molecular weight and molecular weight distribution.[30−38] Therefore, the synthetic challenges have halted further interest in the exploration of side chain ferrocene containing polymers prepared by such conventional polymerization techniques.

Recently, significant attention has been paid again to the first originally developed side chain ferrocene containing polymers, especially well-defined polymers and block copolymers synthesized by controlled and living polymerization such as living anionic polymerization (LAP)[39] and ring-opening metathesis polymerization (ROMP),[40] as well as controlled and living radical polymerization (CRP) techniques[41,42] including atom transfer radical polymerization (ATRP),[43−45] reversible addition–fragmentation chain transfer polymerization (RAFT),[46] and nitroxide-mediated polymerization (NMP).[47] These techniques allow the preparation of polymers with predetermined molecular weight, low polydispersity, high functionality, and diverse architectures.[12,13]

Ring-opening metathesis polymerization (ROMP), a variation of the olefin metathesis reaction, has emerged as a particularly powerful method for synthesizing polymers with tunable sizes, shapes, and functions.[48] It has found a tremendous utility for the synthesis of materials having specific biological, electronic, and mechanical properties. In 1992, the living ROMP was first applied to prepare well-defined side chain ferrocene containing polymers and block copolymers by Schrock and co-workers, who used the molybdenum-based metathesis catalyst [Mo(CH-*t*-Bu)(NAr)(O-*t*-Bu)$_2$] (Figure

Received: July 1, 2014
Published: August 5, 2014

   dx.doi.org/10.1021/om5006897 | *Organometallics* 2014, 33, 4323−4335

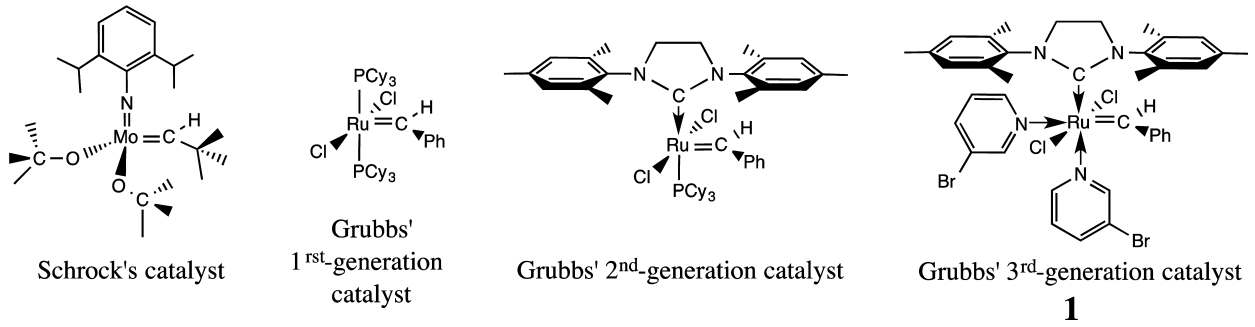

Figure 1. Catalysts successively used for ROMP syntheses of ferrocenyl-containing polymers since 1992 (from left to right).

Scheme 1. Synthesis of Amidoferrocenyl-Containing Homopolymers 6 by ROMP

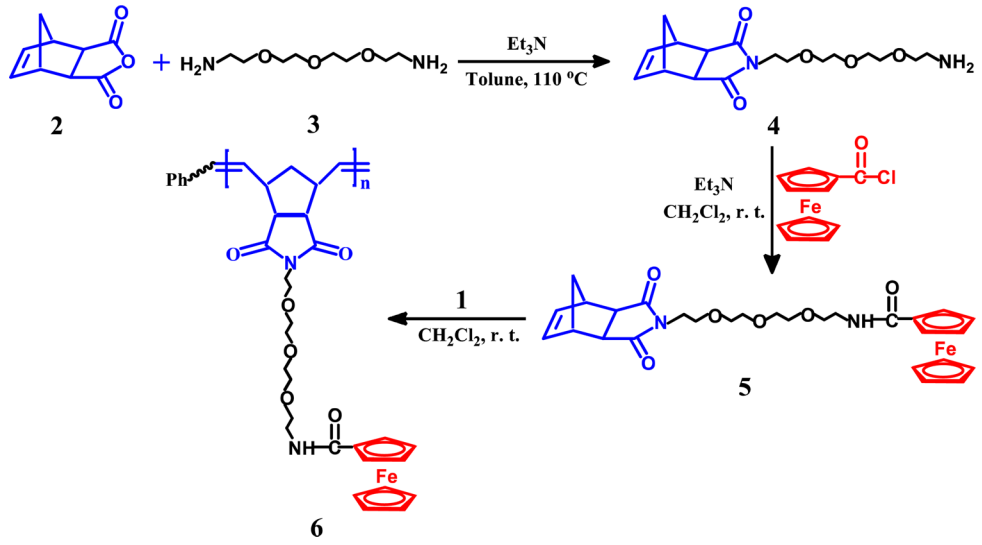

Scheme 2. Synthesis of Amidoferrocenyl-Containing Block Copolymers 10 by ROMP

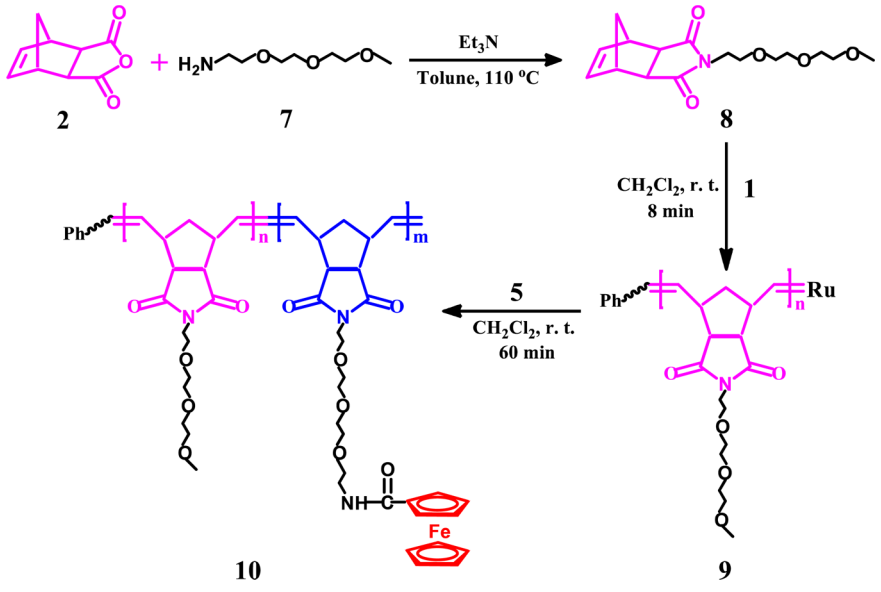

1).[49−51] Since then, the groups of Mirkin,[52−57] Abd-El-Aziz,[58−66] and Luh[67−76] prepared a series of side chain ferrocene containing polynorbornene homopolymers and block copolymers by ROMP. The most frequently used catalysts were ruthenium-based Grubbs first- and second-generation catalysts (Figure 1).[77] Furthermore, although most of the obtained polymers showed low polydispersity, they are often oligomers or polymers with a relatively small number of pendant ferrocenyl units (no more than 30). Up to now, only Tew and co-workers[78] used Grubbs' third-generation catalyst (**1**), shown in Figure 1, a very active catalyst that has a much faster initiation (by at least 3 orders of magnitude) than

dx.doi.org/10.1021/om5006897 | *Organometallics* 2014, 33, 4323−4335

Grubbs' first- and second-generation catalysts.[79,80] Tew's group prepared a series of metal-containing block−random copolymers composed of an alkyl-functionalized homo block (C_{16}) and a random block of cobalt carbonyl (alkyne) units (Co) and ferrocenyl-functionalized (Fe) units via ROMP. These copolymers showed excellent monodispersities (PDI < 1.1) and had the largest theoretical number of ferrocene units of 75. Therefore, these successful results obtained with alkylferrocenyl units opened the route to more work involving *functional* ferrocenyl units and large polymers and the exploration of their properties and applications.

In this work, the very active Grubbs' third-generation ROMP catalyst **1** is used as the initiator (Figure 1).

We present the syntheses and some applications of side chain amidoferrocenyl containing homopolymers (Scheme 1) and block copolymers (Scheme 2) by controlled and living ROMP. Tetraethylene glycol (TEG) was chosen as the linker between the norbornene moiety and amidoferrocenyl units to improve the solubility of macromolecules[81,82] and their biocompatibility that also involves enhanced permeation and retention effects.[82,83] The molecular weights of these new polymers have been well characterized by end-group analysis, MALDI-TOF mass spectra, size exclusion chromatography (SEC), and the Bard−Anson electrochemical method.[84,85] These homopolymers and block copolymers showed an excellent potential in electrode modification resulting from the large polymer sizes and in electrochemical sensing of the ATP^{2-} anion provided by the presence of the amido group on the ferrocenyl moiety that forms efficient hydrogen bonding with oxoanions.[86−88]

2. EXPERIMENTAL SECTION

2.1. General Data. For general data including solvents, apparatuses, compounds, reactions, spectroscopy, CV, and SEC, see the Supporting Information.

2.2. *N*-[11′-Amine-3′,6′,9′-trioxahendecyl]-*cis*-5-norbornene-*exo*-2,3-dicarboximide (4). To a solution of freshly prepared **3** (2.49 g, 12.97 mmol, 5.3 equiv) in toluene (25 mL) was added a solution of **2** (0.4 g, 2.44 mmol, 1 equiv) in toluene (25 mL) dropwise at room temperature over 0.5 h with vigorous stirring. Then, triethylamine (0.2 mL, 1.43 mmol, 0.59 equiv) was added dropwise. The obtained mixture was refluxed for 12 h with a Dean−Stark apparatus before the solvent as well as residual triethylamine were removed via distillation in vacuo. Purification was achieved by column chromatography with dichloromethane (DCM)/methanol (1% → 60%) as eluent, and the product was obtained as a pale yellow oil. Yield: 0.56 g, 68%. ^{1}H NMR of **4** (300 MHz, $CDCl_3$): δ_{ppm} 1.35 (d, J = 10.1 Hz, 1H, CH_2 bridge), 1.48 (d, J = 10.1 Hz, 1H, CH_2-bridge), 1.89 (s, br, 3H, $-NH_2 + H_2O$), 2.68 (d, J = 1.1 Hz, 2H, CO-CH), 2.85 (t, J = 10.6 Hz, 2H, CH_2-NH_2), 3.26 (t, J = 3.4 Hz, 2H, =CH-C*H*), 3.49 (t, J = 10.3 Hz, 2H, $CH_2CH_2NH_2$), 3.57−3.71 (m, 12H, 6 × CH_2), 6.28 (t, J = 3.6 Hz, 2H, CH=CH). ^{13}C NMR of **4** (75 MHz, $CDCl_3$): δ_{ppm} 178.01 (CO-N), 137.79 (C=C), 73.07 ($-CH_2CH_2NH_2$), 70.53, 70.47, 70.205, 69.86 ($-OCH_2CH_2OCH_2CH_2O-$), 66.88 ($-CH_2NH_2$), 47.78 (CO-CH), 45.235 (=CH-CH), 42.675 (CH_2-bridge), 41.45 (CH_2-N-CO), 37.74 (-CH_2CH_2-N-CO). MS (ESI, m/z): calcd for $C_{17}H_{26}N_2O_5$, 338; found, 339.19 (M + H^+).

2.3. *N*-[11′-Ferroceneformamido-3′,6′,9′-trioxahendecyl]-*cis*-5-norbornene-*exo*-2,3-dicarboximide Monomer (5). To a suspension of ferrocenecarboxylic acid (0.5 g, 2.17 mmol) in dry DCM (40 mL) was added dropwise triethylamine (0.1 mL, 0.72 mmol) at room temperature under a nitrogen atmosphere. Then, oxalyl chloride (0.7 mL, 8.2 mmol) was added dropwise at 0 °C. The obtained mixture was stirred overnight at room temperature and dried in vacuo. The residual red solid of crude chlorocarbonyl ferrocene (FcCOCl) was dissolved in dry DCM (20 mL) and added dropwise to a DCM solution (20 mL) of **4** (0.2 g, 0.59 mmol) and triethylamine (1.5 mL, 10.7 mmol). The mixture was stirred overnight under a nitrogen atmosphere at room temperature and then washed with saturated $NaHCO_3$ solution (1 × 100 mL) and distilled water (3 × 100 mL). The organic solution was dried over anhydrous sodium sulfate and filtered, and the solvent was removed in vacuo. The product was purified by column chromatography with DCM/methanol (1% → 20%) as the eluent and obtained as a brown sticky oil. Yield: 0.234 g, 71.8%. ^{1}H NMR of **5** (300 MHz, $CDCl_3$): δ_{ppm} 1.20 (d, J = 9.9 Hz, 1H, CH_2-bridge), 1.32 (d, J = 9.9 Hz, 1H, CH_2-bridge), 2.52 (d, J = 0.9 Hz, 2H, CO-CH), 3.09 (t, J = 3.1 Hz, 2H, =CH-C*H*), 3.41−3.55 (m, 16H, 4 × CH_2CH_2), 4.05 (s, 5H, free Cp), 4.18 (t, J = 3.4 Hz, 2H, sub. Cp), 4.61 (t, J = 3.8 Hz, 2H, sub. Cp), 6.12 (t, J = 3.6 Hz, 2H, CH=CH), 6.59 (t, J = 9.9 Hz, 1H, NHCO). ^{13}C NMR of **5** (50 MHz, $CDCl_3$): δ_{ppm} 177.841 (CON), 170.25 (CONH), 137.71 (CH=CH), 70.375, 70.24, 70.11, 69.975, 69.745, 69.65, 68.20 ($-OCH_2CH_2OCH_2CH_2OCH_2-$, sub. Cp and free Cp), 66.76 (-CH_2NH), 47.68 (CO-CH), 45.14 (=CH-CH), 42.615 (CH_2-bridge), 39.20 (CH_2−NCO), 37.665 ($-CH_2CH_2$-NCO). MS (ESI, m/z): calcd for $C_{28}H_{34}N_2O_6Fe$, 550; found, 573.2 (M + Na^+).

2.4. General Procedure for the Synthesis of Polymeric *N*-[3-(3′,6′,9′-Trioxaundecyl-11′-ferroceneformamido)]-*cis*-5-norbornene-*exo*-2,3-dicarboximide (6) via ROMP. The desired amount of **1** was placed in a small Schlenk flask, flushed with nitrogen, and dissolved in a minimum amount of dry DCM. A known amount of monomer **5** in dry DCM (1 mL per 100 mg of monomer **5**) was added to the catalyst solution under a nitrogen atmosphere with vigorous stirring. The reaction mixture was stirred vigorously for 1 h and then quenched with 0.2 mL of ethyl vinyl ether (EVE). The yellow solid polymers **6** were purified by precipitating in methanol five times and dried in vacuo until constant weight. ^{1}H NMR of **6** (300 MHz, $CDCl_3$): δ_{ppm} 7.23−7.44 (m, phenyl and $CDCl_3$), 6.65 (broad, 1H, NHCO), 5.75 and 5.53 (double broad, 2H, CH=CH), 4.76 (s, 2H, sub. Cp), 4.35 (s, 2H, sub. Cp) (Cp = η^5-C_5H_5), 4.22(s, 5H, free Cp), 3.51−3.67 (broad, 16H, $-CH_2(CH_2OCH_2)_3CH_2-$), 3.26 (broad, =CH-C*H*), 2.71 (broad, CH=CHCHCH_2), 2.13 (broad, CO−CH), 1.61 (broad, CH=CHCHCH_2).

2.5. *N*-[3-(3′,6′,9′-Trioxadecyl)]-*cis*-5-norbornene-*exo*-2,3-dicarboximide Monomer (8). To a solution of freshly prepared 2-(2-(2-methoxyethoxy)ethoxy) ethylamine (7; 1.99 g, 12.21 mmol, 5.0 equiv) in toluene (20 mL) was added dropwise a solution of **2** (0.4 g, 2.44 mmol, 1 equiv) in toluene (25 mL) at room temperature in 0.5 h with vigorous stirring. Then, triethylamine (0.2 mL, 1.43 mmol, 0.59 equiv) was added dropwise. The obtained mixture was refluxed for 12 h with a Dean−Stark apparatus before the solvent as well as residual triethylamine were removed via vacuum distillation. Purification was achieved by column chromatography with DCM/methanol (1% → 50%) as eluent, and the product was obtained as a colorless oil. Yield: 0.65 g, 86.3%. ^{1}H NMR of **8** (300 MHz, $CDCl_3$): δ_{ppm} 1.37 (d, J = 9.6 Hz, 1H, CH_2-bridge), 1.49 (d, J = 9.6 Hz, 1H, CH_2-bridge), 2.69 (d, J = 3.6 Hz, 2H, CO-CH), 3.27 (d, J = 1.8 Hz, 2H, =CH-C*H*), 3.38 (s, J = 4.3 Hz, 3H, CH_3), 3.536−3.683 (m, 12H, 6 × CH_2), 6.23 (t, J = 3.8 Hz, 2H, CH=CH). ^{13}C NMR of **8** (75 MHz, $CDCl_3$): δ_{ppm} 177.45 (CO-N), 137.60 (C=C), 71.657, 70.223, 69.612, 66.53 ($-OCH_2CH_2OCH_2CH_2O-$), 58.64 ($-CH_3$), 47.49 (CO-CH), 45.00 (=CH-CH), 42.464 (CH_2-bridge), 37.47 (N-CH_2CH_2). MS (ESI, m/z): calcd for $C_{16}H_{23}NO_5$, 309; found, 332.2 (M + Na^+).

2.6. General Procedure for the Synthesis of the Block Copolymers 10 by ROMP. The desired amount of **1** was placed in a small Schlenk flask, flushed with nitrogen, and dissolved in a minimum amount of dry DCM. Known amounts of monomers **8** and **5** were placed in two small glass tubes, respectively, and dissolved in dry DCM (1 mL per 100 mg of monomers). First, the monomer **8** was transferred to the flask containing **1** via a syringe. The reaction mixture was stirred vigorously for 8 min, and a known amount of the reaction solution was taken out and quenched with 0.1 mL of ethyl vinyl ether (EVE) for ^{1}H NMR analysis. Then, the solution containing monomer **5** was transferred to the reaction flask via a syringe. The polymerization was allowed to continue for 60 min and quenched with 0.2 mL of ethyl EVE. The copolymers **10** were purified by precipitation in diethyl ether five times and dried in vacuo to constant

dx.doi.org/10.1021/om5006897 | *Organometallics* 2014, 33, 4323−4335

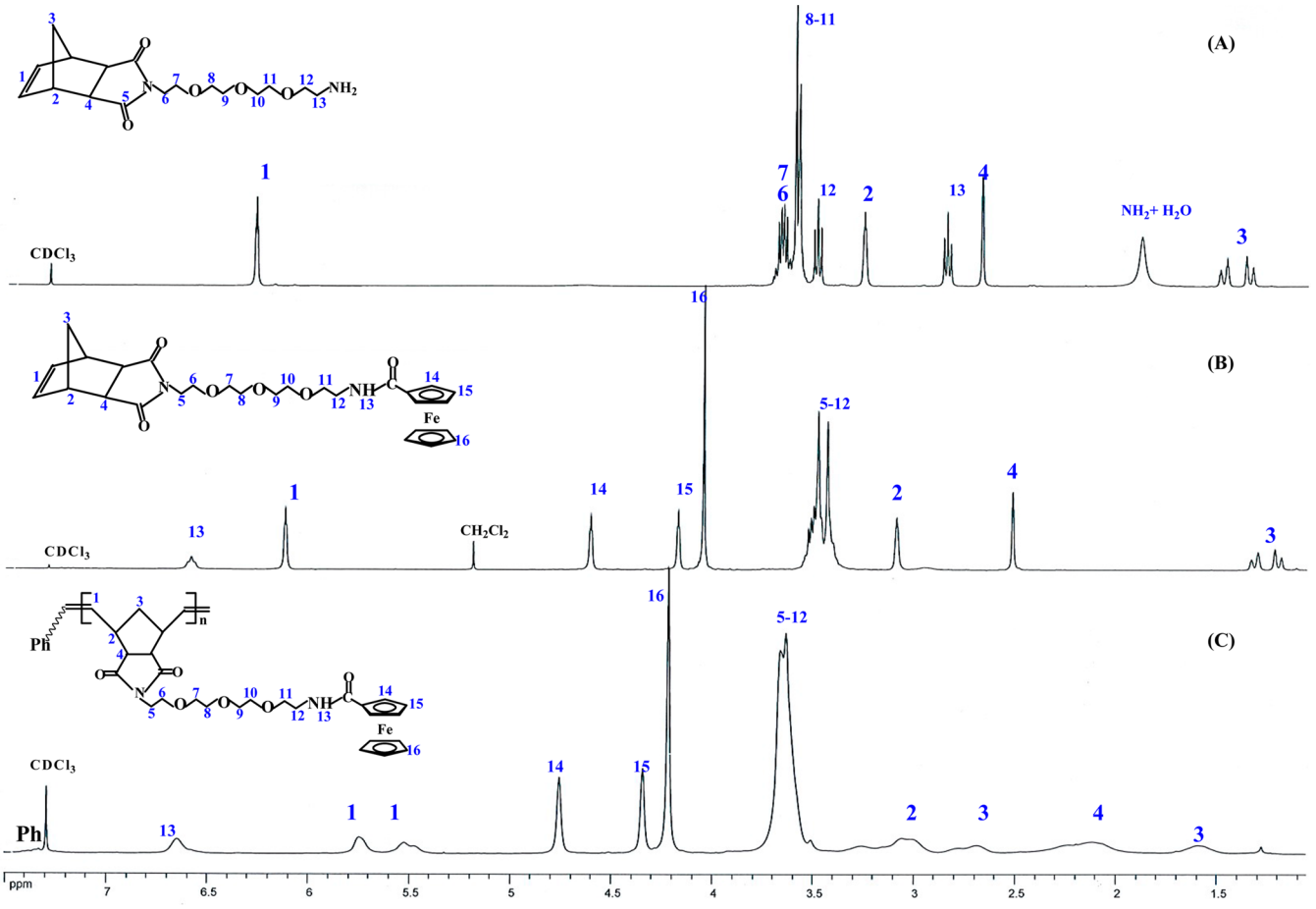

Figure 2. ^{1}H NMR spectra of **4** (A), monomer **5** (B), and polymer **6** (C) in $CDCl_3$.

weight. ^{1}H NMR of polymers **9** (300 MHz, $CDCl_3$): δ_{ppm} 7.190−7.354 (m, phenyl and $CDCl_3$), 5.751 and 5.508 (broad doublet, 2H, CH═CH), 3.521−3.595 (broad, 12H, $-CH_2(CH_2OCH_2)_2CH_2-$), 3.355 (s, 3H, OCH_3), 3.043 (broad, ═CH-C*H*), 2.683 (broad, CH═CHCHCH_2), 2.070 (broad, CO-CH), 1.578 (broad, CH═CHCHCH_2). ^{1}H NMR of copolymers **10** (300 MHz, $CDCl_3$): δ_{ppm} 7.26−7.36 (m, phenyl and $CDCl_3$), 6.47 (broad, NHCO), 5.75 and 5.50 (broad doublet, CH═CH), 4.71 (s, sub. Cp), 4.32 (s, sub. Cp), 4.19 (s, free Cp), 3.52−3.60 (broad, $-CH_2(CH_2OCH_2)_2CH_2-$ and $-CH_2(CH_2OCH_2)_3CH_2-$), 3.355 (s, OCH_3), 3.04 (broad, ═CH-C*H*), 2.68 (broad, CH═CHCHCH_2), 2.08 (broad, CO-CH), 1.575 (broad, CH═CHCHCH_2).

2.7. Electrochemistry, Modified Electrodes, and Redox Sensing. All electrochemical measurements were recorded under a nitrogen atmosphere. Conditions: solvent, dry dichloromethane; temperature, 20 °C; supporting electrolyte, [nBu$_4$N][PF$_6$] 0.1 M; working and counter electrodes, Pt; reference electrode, Ag; internal reference, FeCp*$_2$ (Cp* = η^5-C$_5$Me$_5$); scan rate, 0.200 V s^{-1}. The number of electrons involved in the oxidation wave of ferrocenyl polymers was calculated by the Bard−Anson equation: $n_p = (i_{dp}/C_p)/(i_{dm}/C_m)(M_p/M_m)^{0.775}$ (see text and the Supporting Information). The experiments were conducted by adding a known amount of polymer (see the Supporting Information) in 3 mL of dry DCM, and then a known amount of [FeCp*$_2$] (see the Supporting Information) in 2 mL of DCM was added to the solution. After the CVs were recorded, the intensities of the oxidation waves of the polymers and of the internal reference [FeCp*$_2$] were measured. The values were introduced in the above equation, giving the final number of electrons (n_p). The modified electrodes were prepared after approximately 25 adsorption cycles around the ferrocenyl potential on Pt electrodes. Their electrochemical behavior was checked in 5 mL of a DCM solution containing only [nBu$_4$N][PF$_6$] 0.1 M at various scan rates: 25, 50, 100, 200, 300, 400, 500, and 600 mV s^{-1}. Redox recognition was conducted in two different ways. (a) In solution via titration: the CVs were recorded upon addition of 0, 0.25, and 0.5 equiv of [n-Bu$_4$N]$_2$[ATP]. The potentials of the new wave were measured using [FeCp*$_2$] as an internal reference. (b) With modified electrodes: the CVs were recorded upon addition of [n-Bu$_4$N]$_2$[ATP] to an electrochemical cell containing a Pt-modified electrode.

3. RESULTS AND DISCUSSION

3.1. Synthesis and ROMP of the Amidoferrocenyl-Containing Monomer 5. As shown in Scheme 1, the new amidoferrocenyl-containing monomer **5** was prepared by an amidation reaction between ferrocenylcarbonyl chloride and the key intermediate *N*-[11′-amine-3′,6′,9′-trioxahendecyl]-*cis*-5-norbornene-*exo*-2,3-dicarboximide (**4**). This compound **4** was prepared from *cis*-5-norbornene-*exo*-2,3-dicarboxylic anhydride (**2**) in the presence of 1,11-diamine-3,6,9-trioxaundecane (**3**), whose method of synthesis is well described in the Supporting Information. Figure 2A shows the ^{1}H NMR spectrum of the intermediate **4**. The peak at 6.28 ppm corresponds to the olefinic protons, while the two double peaks at 1.36−1.37 and 1.46−1.50 ppm originate from the characteristic bridge-methylene protons of the *cis*-norbornene structure. As shown in the ^{1}H NMR spectrum of monomer **5** (Figure 2B), the appearance of the amido proton at 6.59 ppm and the three characteristic cyclopentadienyl (Cp) protons at 4.61, 4.18, and 4.05 ppm, respectively, demonstrate the success of the amidation reaction. The methylene protons of the TEG linker are concentrated at 3.41−3.53 ppm, which is different from the

dx.doi.org/10.1021/om5006897 | *Organometallics* 2014, 33, 4323−4335

Table 1. Molecular Weight Data for the Amidoferrocenyl-Containing Polymer 6

	$[M_5]:[C]^a$				
	5:1	16:1	50:1	100:1	400:1
conversn (%)[b]	>99	>99	>99	>99	83
n_{p1}[c]	5 ± 1	16 ± 2	50 ± 5	95 ± 5	332
n_{p2}[d]	4.2 ± 0.4	14 ± 1	34 ± 2	51 ± 3	64 ± 3
n_{p3}[e]	4 ± 0.1	15 ± 1	47 ± 3	94 ± 5	336 ± 8
M_n[f]	2854	8904	27604	55104	182704
M_n[g]	2878.7	8930.2			
M_n[h]	1417	4239	5508		
PDI[h]	1.09	1.08	1.03		

[a] $[M_5]:[C]$ is the molar feed ratio of monomer **5** and **1**. [b] Monomer conversion determined by ^{1}H NMR. [c] Degree of polymerization obtained from ^{1}H NMR using conversion of monomer **5**. [d] Degree of polymerization determined via end-group analysis by ^{1}H NMR spectroscopy in CD_2Cl_2. [e] Degree of polymerization determined by the Bard–Anson electrochemical method. [f] MWs obtained by ^{1}H NMR using conversion of monomer **5**. [g] MWs ($+Na^+$) determined via MALDI-TOF mass spectroscopy. [h] Obtained from SEC using polystyrenes as standards.

dispersed distribution in intermediate **4**. All of the other peaks are clearly assigned. ^{13}C NMR and mass spectroscopy (Figures S6 and S7, Supporting Information) further confirm the structure of the monomer **5**.

The preparation of amidoferrocenyl-containing polymers **6** by ROMP was carried out in dry DCM at room temperature using catalyst **1**. As shown in Figure 2C, the disappearance of the peak at 6.13 ppm corresponding to the olefinic protons of monomer **5** and the appearance of new two broad peaks at 5.53 and 5.75 ppm that arise from the olefinic protons of polymers **6** indicate the successful polymerization of the monomer **5**. Furthermore, the other peaks of the *cis*-norbornene backbone in polymers **6** change into broad signals that are very different from the sharp signals of the monomers.

In this study, a series of amidoferrocenyl-containing homopolymers **6** were synthesized with molar feed ratios of monomer to catalyst from 5:1 to 400:1. In situ ^{1}H NMR analysis of the crude reaction mixture indicated that the monomer conversions, which were calculated by comparing the ^{1}H NMR signals of the olefinic protons between monomer **5** (6.13 ppm) and the polymers **6** (5.53 and 5.75 ppm), were nearly 100% within 60 min when the molar feed ratio was less than 50. It was necessary to extend the polymerization time in order to obtain the larger polymers. For instance, when the molar feed ratio was 100:1, the monomer conversion was only 50% after 60 min but improved to nearly 100% after overnight stirring. For the largest molar feed ratio of 400:1, the monomer conversion only reached 83% even after 4 days. The amidoferrocenyl-containing homopolymers **6** are not soluble in organic solvents such as acetone, acetonitrile, methanol, and diethyl ether, unlike the monomer **5**, but they are soluble in dichloromethane, chloroform, tetrahydrofuran (THF), and strongly polar solvents such as DMF and dimethyl sulfoxide (DMSO). The smaller polymers have better solubilities than the larger polymers. For instance, the polymer **6** with a molar feed ratio of 50:1 is partially soluble in THF, but when the

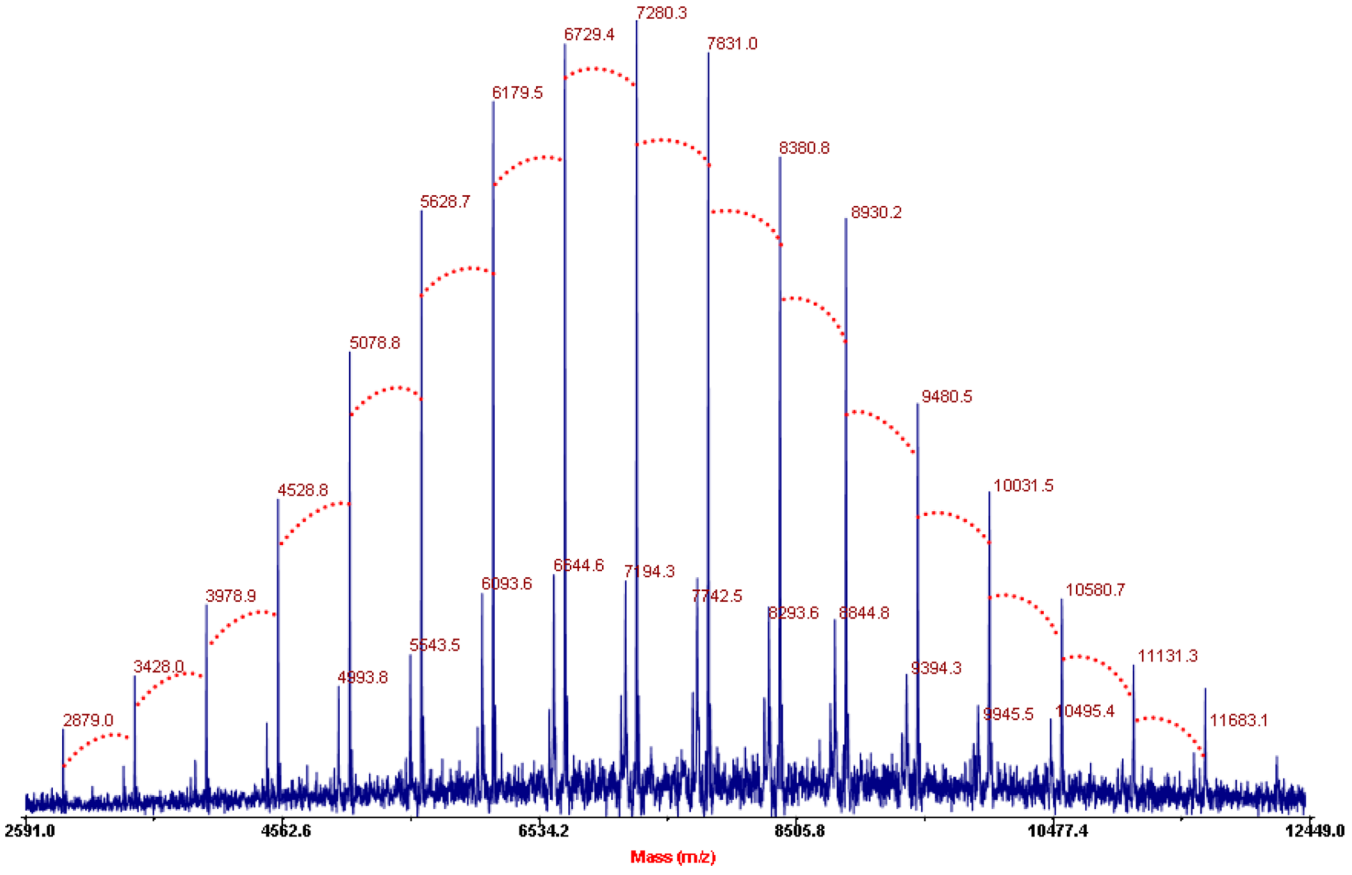

Figure 3. MALDI-TOF MS spectrum of polymer **6**[16]. The molar feed ratio of monomer **5** to **1** is 16:1. The red dotted lines correspond to the difference between molecular peaks of a value of 550 ± 1 Da (MW of **5**).

dx.doi.org/10.1021/om5006897 | *Organometallics* 2014, 33, 4323–4335

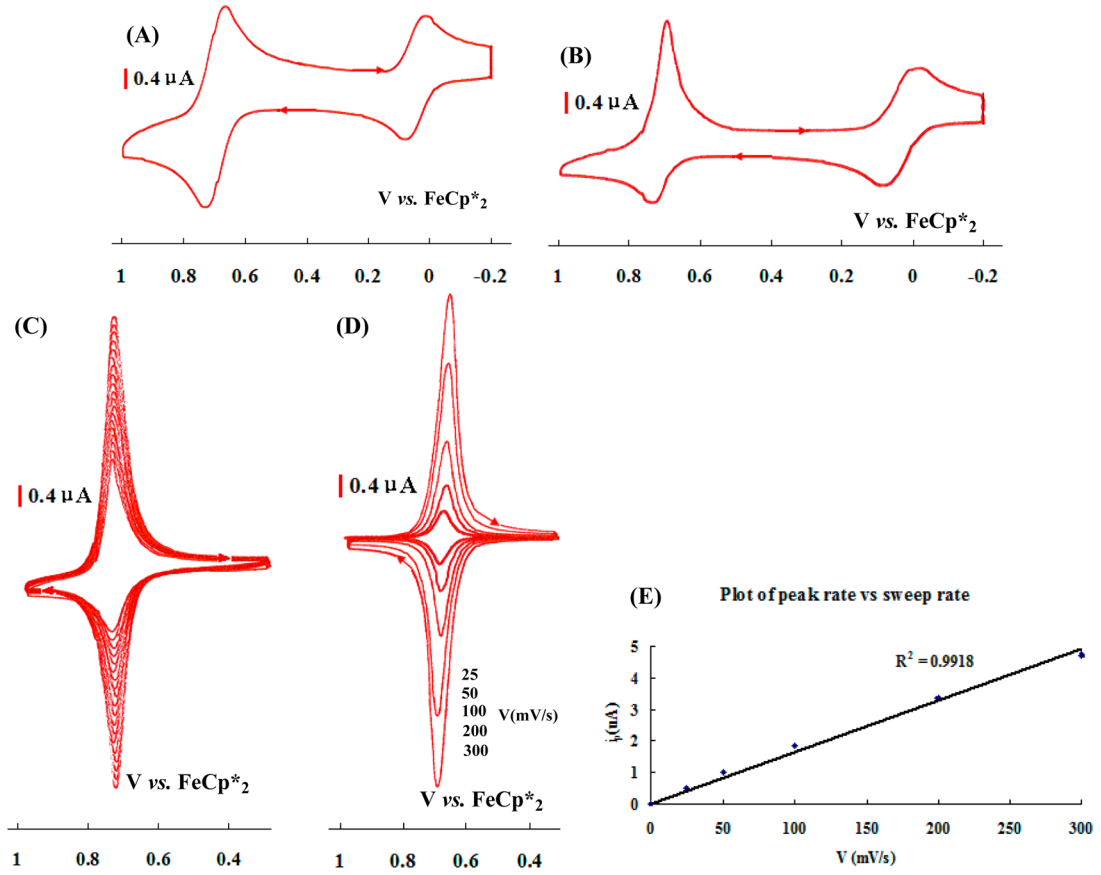

Figure 4. Electrochemical properties of monomer **5** and polymer $\mathbf{6}^{50}$. The molar feed ratio of monomer **5** to **1** is 50:1. (A) CV of monomer **5** in CH_2Cl_2: internal reference, $FeCp^*_2$; reference electrode, Ag; working and counter electrodes, Pt; scan rate, 0.4 mV/s; supporting electrolyte, [*n*-Bu_4N][PF_6]. The wave at 0.0 V is that of the reference [$FeCp^*_2$]. (B) CV of the polymer $\mathbf{6}^{50}$ in CH_2Cl_2: internal reference, [$FeCp^*_2$]; reference electrode, Ag; working and counter electrodes, Pt; scan rate, 0.2 mV/s; supporting electrolyte, [*n*-Bu_4N][PF_6]. The wave at 0.0 V is that of the reference [$FeCp^*_2$]. (C) Progressive adsorption of the polymer $\mathbf{6}^{50}$ upon scanning around the ferrocenyl area. (D) Pt electrode modified with the polymer $\mathbf{6}^{50}$ at various scan rates in CH_2Cl_2 solution (containing only the supporting electrolyte). (E) Intensity as a function of scan rate (linearity shows the expected behavior of the absorbed polymer).

Table 2. Redox Potentials and Chemical (i_c/i_a) and Electrochemical ($E_{pa} - E_{pc} = \Delta E$) Reversibilities for Monomer 5, Polymers 6, and Corresponding Modified Electrodes

			modified electrode		
compd	$E_{1/2}$ (ΔE) (mV)	i_c/i_a	$E_{1/2}$ (ΔE) (mV)	Γ (mol/cm^2)[a]	Γ (mol/cm^2)[a] (ferrocenyl sites)
monomer **5**	680 (70)	1.0			
polymer $\mathbf{6}^{16}$	680 (30)	2.2	660 (0)	5.52×10^{-11}	8.27×10^{-10}
polymer $\mathbf{6}^{50}$	680 (40)	3.1	660 (0)	4.53×10^{-11}	2.13×10^{-9}
polymer $\mathbf{6}^{100}$	680 (30)	2.2	660 (0)	3.11×10^{-11}	2.92×10^{-9}
polymer $\mathbf{6}^{400}$	680 (40)	2.5	660 (0)	1.30×10^{-11}	4.40×10^{-9}

[a]Surface coverage on the modified Pt electrode obtained after approximately 25 adsorption cycles.

molar feed ratio is increased to 100:1, the polymer **6** is insoluble in THF.

3.2. Molecular Weight Analysis of the Polymers 6. Molecular weights (MWs) can be measured via a variety of techniques, including gel permeation chromatography (GPC), osmometry, static light scattering, matrix-assisted laser desorption-ionization time-of-flight mass spectrometry (MALDI-TOF MS), viscometry, small-angle X-ray scattering, small-angle neutron scattering, ultracentrifugation, cryoscopy, ebulliometry, and end-group analysis.[86] Each method has its respective advantages and disadvantages, and the most suitable methods also depend on the polymer type. In this study, size exclusion chromatography (SEC), MALDI-TOF MS, end-group analysis, and the Bard–Anson electrochemical method[84,85] were used to investigate the MWs of the amidoferrocenyl-containing polymers **6**.

As shown in Table 1, the theoretical MWs and polymerization degrees of the polymers **6** were calculated according to the molar feed ratios and the corresponding monomer conversions from ^{1}H NMR. End-group analysis by ^{1}H NMR of the polymers **6** in CD_2Cl_2 (see Figure S10, Supporting Information) was conducted by comparing the five protons of end-group phenyls (7.20–7.43 ppm) with amido protons (6.59 ppm), olefinic protons (5.56 and 5.77 ppm), Cp protons (4.23, 4.37, and 4.74 ppm), and linker protons (3.55–3.65 ppm), respectively. For the small polymers in which theoretical MWs

dx.doi.org/10.1021/om5006897 | *Organometallics* 2014, 33, 4323–4335

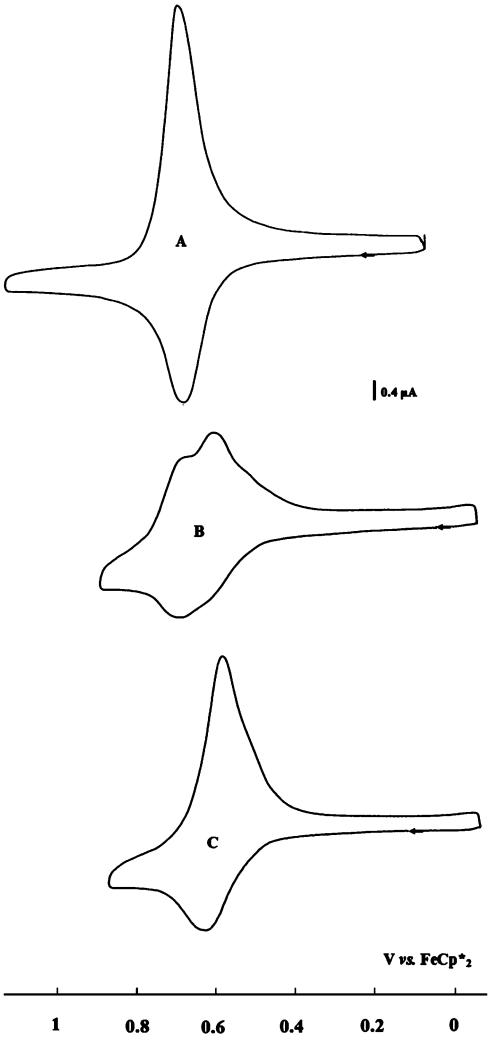

Figure 5. CVs for the titration of $[n\text{-}Bu_4N]_2[ATP]$ with polymer **6**[50] in CH_2Cl_2 at 20 °C by adding the salt of the anion to the polymer solution: (A) before addition of $[n\text{-}Bu_4N]_2[ATP]$; (B) during the titration with 0.25 equiv of $[n\text{-}Bu_4N]_2[ATP]$; (C) with 0.5 equiv of $[n\text{-}Bu_4N]_2[ATP]$.

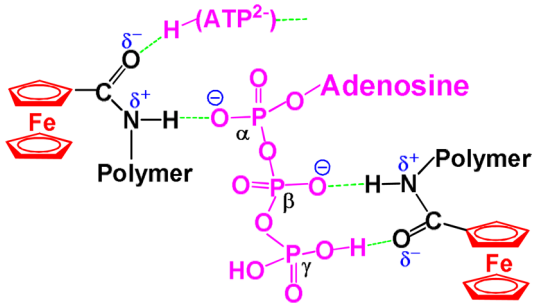

Figure 6. Hydrogen-bonding interactions between ATP^{2-} and two amidoferrocenyl groups of polymers **6**.

were less than 10000 Da, the MWs by NMR conversion and end-group analysis were in good agreement, which was further confirmed by MALDI-TOF MS results (Figure 3 and Figure S13 (Supporting Information)). As shown in Figure 3, the MALDI-TOF mass spectrum of polymer **6**[16] showed well-defined individual peaks for polymer fragments that are separated by 550 ± 1 Da corresponding to the mass of one

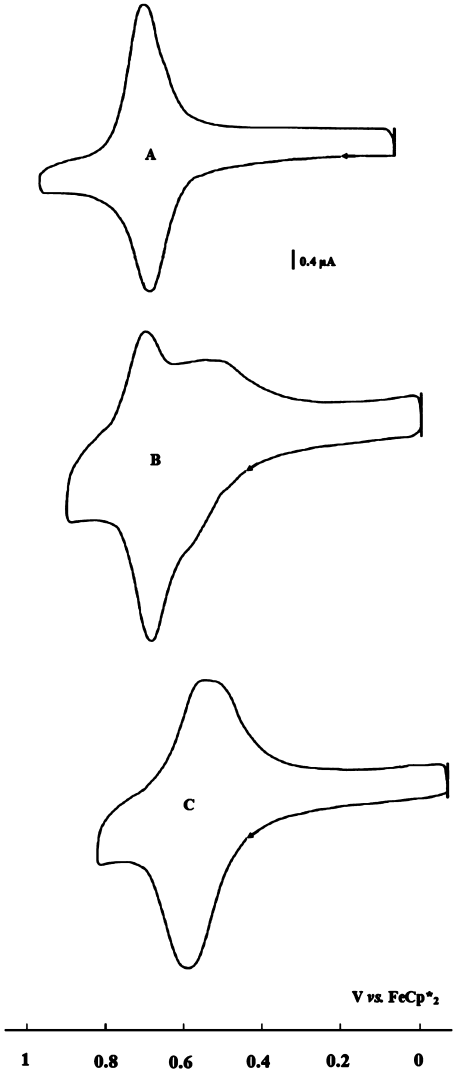

Figure 7. CVs for the titration of $[n\text{-}Bu_4N]_2[ATP]$ by the modified Pt electrode with polymer **6**[50] in CH_2Cl_2 at 20 °C: (A) before addition of $[n\text{-}Bu_4N]_2[ATP]$; (B) during titration of $[n\text{-}Bu_4N]_2[ATP]$; (C) after addition of excess $[n\text{-}Bu_4N]_2[ATP]$.

monomer **5** unit. There is a peak at 8930.2 Da that corresponds to the molecular weight of $(C_6H_6)(C_{28}H_{34}N_2O_6Fe)_{16}(C_2H_2)$-Na. On the other hand, the MWs obtained by SEC were always smaller than the theoretical values, which may result from the obvious structural difference between the polystyrene standards and the amidoferrocenyl-containing polymers **6**. However, none the polydispersity indexes (PDI) obtained by SEC traces were larger than 1.1, which demonstrated a controlled polymerization.

End-group analysis and MALDI-TOF MS are not reliable for the large polymers, however. The SEC traces of the large polymers **6** could not be obtained in THF because of solubility problems. SEC measurements were also attempted in $CHCl_3$, but no signal was observed, probably because of the strong adsorption of the large polymers **6** on the column stationary phase. From the DOSY ^1H NMR spectra of the polymers **6** (Figure S14–S16, Supporting Information), the hydrodynamic diameters of polymers **6** can be calculated using the Stokes–Einstein equation (see Supporting Information). A progressive increase of the hydrodynamic diameters was observed upon increasing the molar feed ratio of monomer **5** to **1** from 50:1 to

dx.doi.org/10.1021/om5006897 | *Organometallics* 2014, 33, 4323–4335

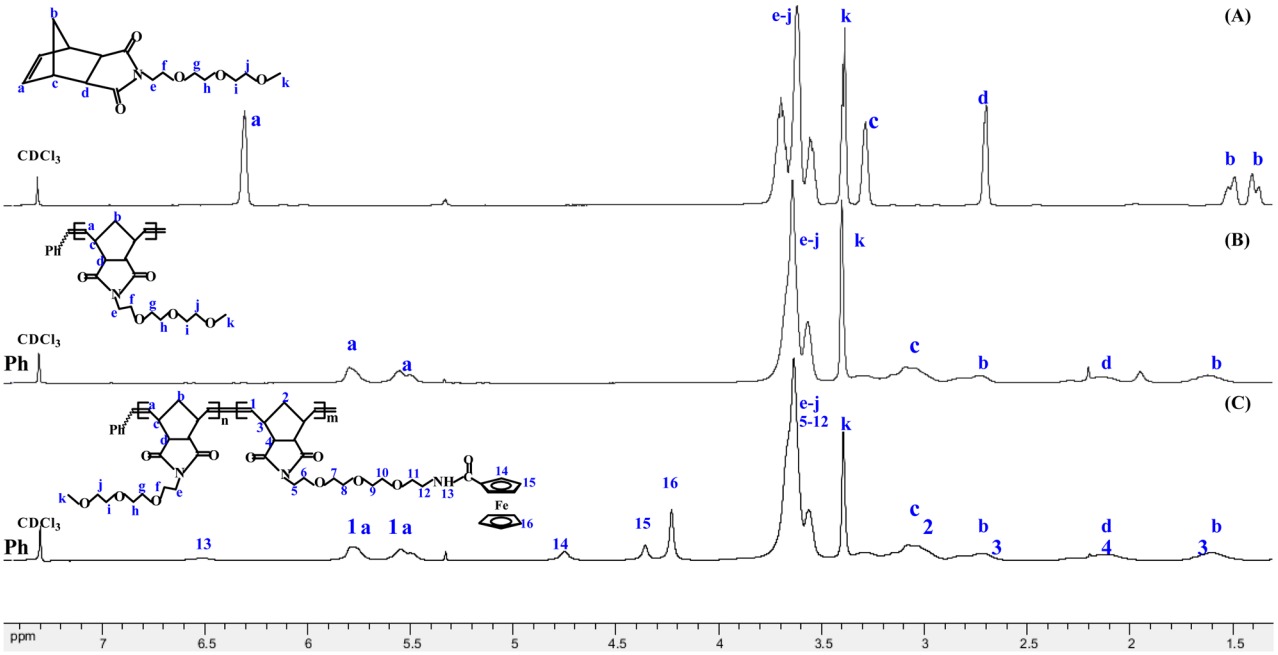

Figure 8. ^{1}H NMR spectra of monomer **8** (A), polymer **9** (B), and copolymer **10** (C) in $CDCl_3$.

Table 3. Molecular Weight Data of the Amidoferrocenyl-Containing Block Copolymers 10

	$[M_8]$:$[M_5]$:$[C]^a$			
	6:3:1	20:10:1	100:50:1	100:100:1
conversn (%)^b	>99	>99	>99	>99
$n_{p1}{}^c$	3	10	50	100
$n_{p2}{}^d$	3 ± 0.3	10 ± 1	44 ± 3	82 ± 5
$n_{p3}{}^e$	2.7 ± 0.3	9 ± 1	44 ± 3	98 ± 3
$M_n{}^f$	3608	11784	58504	86004
$M_n{}^g$	3633.9			
$M_n{}^h$	2585	7139	25454	22325
PDI^h	1.10	1.06	1.14	1.11

^{a}[M_8]:[M_5]:[C]: molar feed ratio of monomer **8**, monomer **5**, and **1**. ^{b}Monomer conversion of monomer **5** determined by ^{1}H NMR. ^{c}Degree of polymerization obtained from ^{1}H NMR using conversion of the amidoferrocenyl-containing monomer **5**. ^{d}Degree of polymerization for the amidoferrocenyl-containing block determined via end-group analysis by ^{1}H NMR spectroscopy. ^{e}Degree of polymerization for the amidoferrocenyl-containing monomer **5** determined by the Bard–Anson electrochemical method. ^{f}MWs obtained for copolymers **10** by ^{1}H NMR using conversion of monomers **8** and **5**. ^{g}MWs (+Na^+) determined by MALDI-TOF mass spectroscopy. ^{h}Obtained from SEC using polystyrenes as standards.

400:1, which indicates a concomitant increase of MWs. Although the DOSY results cannot quantitatively characterize the polydispersity of polymers, the low deviation values of the diffusion coefficient (D) from different DOSY ^{1}H NMR peaks show that these polymers should have a narrow molecular weight distribution.

In order to further characterize the polymers **6**, especially the large ones, we have used the Bard–Anson electrochemical method,[84,85] in which the compared intensities in the cyclic voltammograms (CVs) of the polymers and monomer were used. The total number of electrons transferred in the oxidation wave for the polymer (n_p) is the same as that of monomer units in the polymer, because only one electron from Fe^{II} (ferrocene) to Fe^{III} (ferrocenium) is transferred from each monomer unit to the anode during the electrochemical experiment. This number n_p is estimated by employing the Bard–Anson empirical equation[84,85] previously derived for conventional polarography, where i_d, M, and C are the CV wave intensity of the diffusion current, molecular weight, and concentration of the monomer (m) and polymer (p), respectively:

$$n_p = \frac{(i_{dp}/C_p)}{(i_{dm}/C_m)}\left(\frac{M_p}{M_m}\right)^{0.275}$$

As shown in Table 1, the estimated values of electrons (n_{p3}) for all of the polymers **6** showed excellent consistency with the polymerization degree (n_{p1}) obtained from ^{1}H NMR, which further demonstrated the controlled characteristic for the ROMP of the amidoferrocenyl-containing monomer **5**. For example, for the polymer $\mathbf{6}^{400}$, the largest polymer prepared in this study, the calculated polymerization degree (n_{p1}) from the conversion rate is 332, and the value of n_{p2} from end-group analysis is 64 ± 3, but the n_{p3} value from the above formula is 336 ± 8, which is very close to the theoretical result. Thus, the Bard–Anson electrochemical method is a valuable tool to check the n_p and MW values of amidoferrocenyl containing polymers **6**.

3.3. Redox Properties of Polymers 6 and Electrochemical Sensing of ATP^{2-}. The new ferrocenyl monomer **5** and the side chain amidoferrocenyl containing homopolymers **6** have been studied by CV[87–90] using decamethylferrocene [$FeCp^*_2$] as the internal reference.[90] The CVs have been recorded in DCM (Figure 4 and Figures S20 and S21 (Supporting Information)), and the $E_{1/2}$ data (measured vs [$FeCp^*_2$]) are gathered in Table 2. For monomer **5** and all of the polymers **6**, a single oxidation wave is observed for all the ferrocenyl groups, and this single wave is marred by adsorption of the polymer onto the electrode. For the monomer **5**, the $Fe^{III/II}$ oxidation potential of the ferrocenyl redox center is around 680 mV, whereas for polymers **6** the potentials are also around 680 mV, although the precise value is to a certain extent not as precise due to the adsorption (Figure 4B).

dx.doi.org/10.1021/om5006897 | Organometallics 2014, 33, 4323–4335

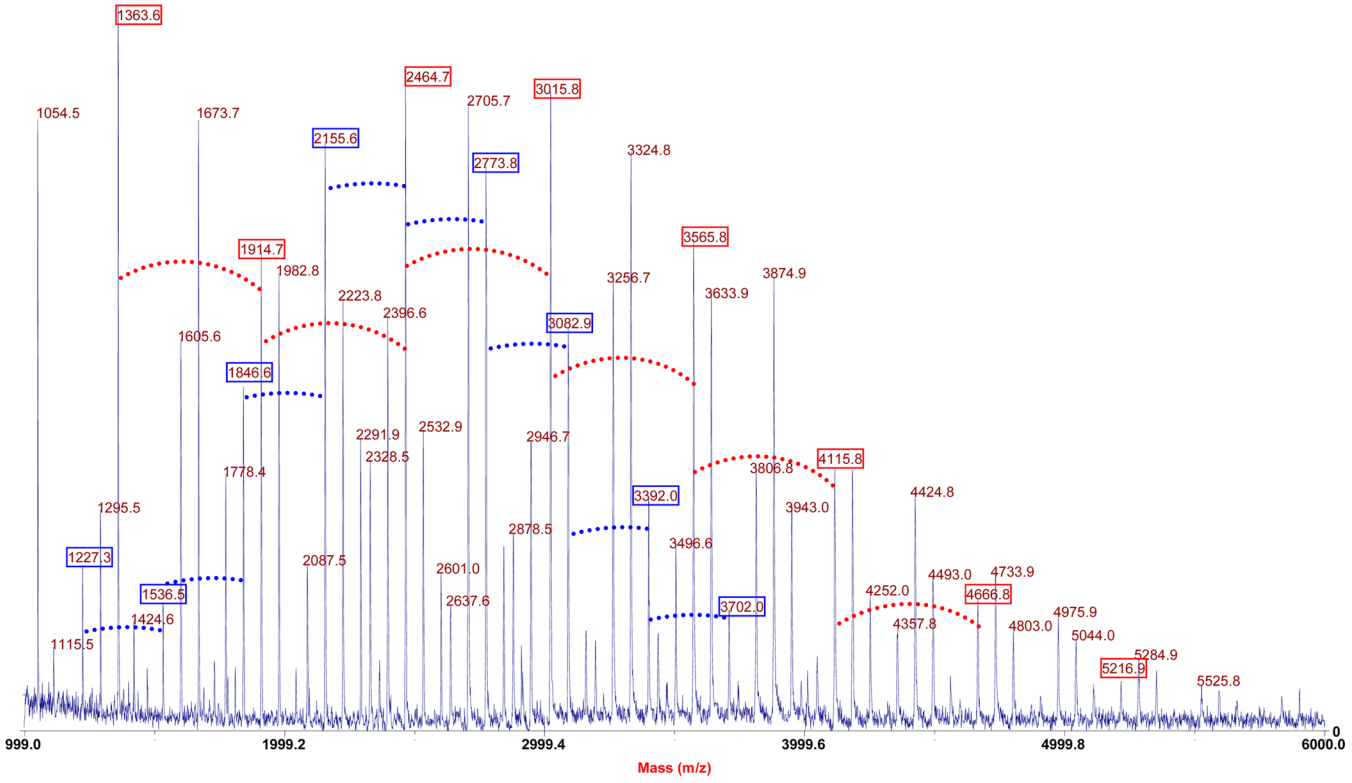

Figure 9. MALDI-TOF MS spectrum of the copolymer $\mathbf{10}^{6/3}$. The molar feed ratio of monomers **8** and **5** to **1** is 6:3:1. The dotted red and blue lines correspond to the difference between molecular peaks of 550 ± 1 (MW of **5**) and 309 ± 1 Da (MW of **8**), respectively.

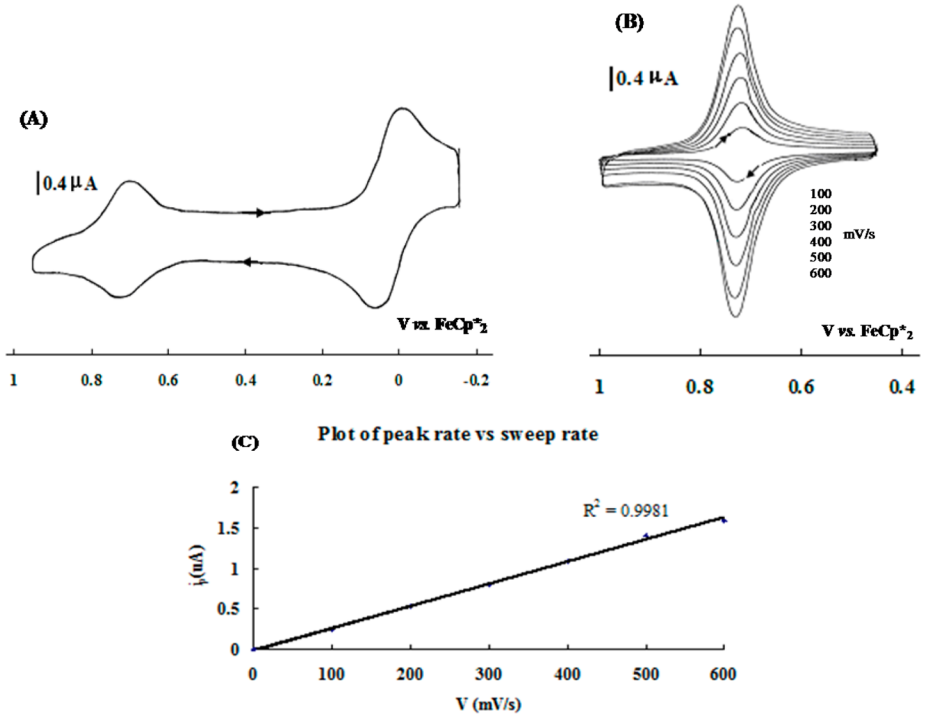

Figure 10. Electrochemical properties of the copolymer $\mathbf{10}^{100/50}$. The molar feed ratio of monomers **8** and **5** to **1** is 100:50:1. (A) CV of the copolymer in DCM: internal reference, [$FeCp^*_2$]; reference electrode, Ag; working and counter electrodes, Pt; scan rate, 0.4 mV/s; supporting electrolyte, [n-Bu_4N][PF_6]. (B) Pt electrode modified by the copolymer at various scan rates in DCM solution containing only the supporting electrolyte. (C) Intensity as a function of scan rate (the linearity shows the expected behavior of the adsorbed polymer).

There was no adsorption phenomenon during CV for monomer **5**, but for all the polymers **6** obvious and strong adsorption onto electrodes was observed, as shown in Figure 4C, upon scanning around the oxidation potential of the amidoferrocenyl group. The progressive adsorption onto electrodes is an advantage for the facile formation of robust

dx.doi.org/10.1021/om5006897 | *Organometallics* 2014, 33, 4323−4335

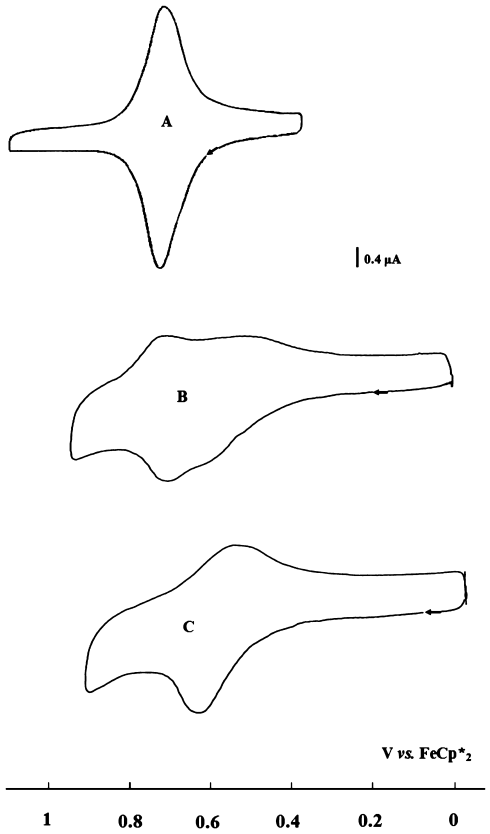

Figure 11. CVs for the titration of $[n\text{-}Bu_4N]_2[ATP]$ by the Pt electrode modified with the copolymer $\mathbf{10}^{100/50}$ in DCM at 20 °C: (A) before addition of $[n\text{-}Bu_4N]_2[ATP]$; (B) during addition of $[n\text{-}Bu_4N]_2[ATP]$; (C) after addition of excess $[n\text{-}Bu_4N]_2[ATP]$.

metallopolymer-modified electrodes upon scanning around the amidoferrocenyl potential zone.[87−90] Modification of electrodes using polymers **6** with various MWs has been successful, resulting in detectable electroactive materials. The electrochemical behavior of the modified electrodes was studied in DCM containing only the supporting electrolyte (Figure 4D). A well-defined symmetrical redox wave is observed that is characteristic of a surface-confined redox couple, with the expected linear relationship of peak current with potential sweep rate (Figure 4E).[87] The modified electrode is stable, as repeated scanning does not modify the CVs. Furthermore, no splitting between oxidation and reduction peaks is observed (ΔE = 0 mV), which suggests that no structural change takes place within the electrochemical redox process.[85,87] These Pt electrodes modified by polymers **6** are durable and reproducible, as no loss of electroactivity is observed after scanning several times or after standing in air for several days. The surface coverages of the electroactive amidoferrocenyl sites of the modified electrodes for all the polymers are given in Table 2.

Oxoanion sensing is a key field of molecular recognition,[91−93] in particular because DNA fragments include adenosine triphosphate anion (ATP^{2-}), an important coenzyme that transports chemical energy to cells for metabolism. Here electrochemical recognition of ATP^{2-} by the redox-active polymers was studied first in dichloromethane (DCM) solution using the *n*-butylammonium salt $[n\text{-}Bu_4N]_2[ATP]$ and then using a modified electrode that was derivatized by adsorption of the polymers. Let us first examine the redox recognition in solution. Addition of $[n\text{-}Bu_4N]_2[ATP]$ to an electrochemical cell containing a solution of polymer $\mathbf{6}^{50}$ in DCM led to the appearance of a new wave at a potential less positive than the initial wave, the intensity of which decreased while that of the new wave increased (Figure 5). Indeed, the interaction of the anions with redox groups releases electron density, rendering oxidation of the amidoferrocenyl group easier. The difference in amidoferrocenyl redox potential between the initial wave and the new wave (ΔE) is 70 mV. The equivalence point is reached when 0.5 equiv of $[n\text{Bu}_4N]_2[ATP]$ has been added (Figure 5C), which is in accord with the double negative charge of this anion and signifies that the ATP^{2-} anion is quantitatively recognized by the polymer $\mathbf{6}^{50}$ in DCM solution and that two amidoferrocenyl groups are interacting with each ATP^{2-}.

The α and β phosphates near the ribose are those that were found by the group of Hampe and Kappes using infrared multiple photon dissociation and photoelectron spectroscopy to bear the two negative charges of ATP^{2-}.[94] Accordingly, the stoichiometry of the titration that corresponds to two amidoferrocenyl units per ATP^{2-} is dictated by the interactions of these two negatively charged α and β phosphates with the NH groups of amidoferrocenyl units. In the oxidized ferrocenium form generated at the anode, the interaction of the oxygen anions involves an NH group of considerably increased acidity due to the positive charge that is delocalized over the amidoferrocenium moiety. The H bond is then strengthened, and the synergy between this H bond and the electrostatic bond between the cation and the anion is sufficiently strong to significantly modify the ferrocenyl redox potential. The two negatively charged phosphates are very different from each other (Figure 6): the β and γ phosphates form a favorable chelating double H bond with an amidoferrocenyl group of polymers **6** ("intramolecular H bonding"), whereas the α phosphate can only form a single H bond with another amidoferrocenyl group. This group also forms another H bond between its carbonyl group and another ATP^{2-} molecule ("intermolecular" H bonding), as shown in Figure 6.

The Pt electrode modified with the polymer $\mathbf{6}^{50}$ was also used for its recognition in DCM solution containing only $[n\text{-}Bu_4N][PF_6]$ as the supporting electrolyte, and a similar trend was observed. As shown in Figure 7, the addition of $[n\text{-}Bu_4N]_2[ATP]$ to an electrochemical cell containing the modified Pt electrode in DCM caused the appearance of a new wave at a potential less positive than that for the initial wave. The intensity of the initial wave decreased, while that of the new wave increased. The difference in ferrocenyl redox potential between the initial wave and the new wave (ΔE) is 130 mV: i.e., 60 mV larger than that observed with polymer $\mathbf{6}^{50}$ in solution. The larger ΔE value signifies a rather strong interaction of the amidoferrocenium group on the modified Pt electrode with the ATP^{2-} anions. Consequently, the modified Pt electrode with polymer $\mathbf{6}^{50}$ is a good candidate for the qualitative recognition of ATP^{2-} anions.[91−93]

3.4. Synthesis of the Amidoferrocenyl Block Copolymers 10. As shown in Scheme 2, first the new monomer *N*-[3-(3′,6′,9′-trioxadecyl)]-*cis*-5-norbornene-*exo*-2,3-dicarboximide (**8**) was synthesized by reaction between **2** and 2-(2-(2-methoxyethoxy)ethoxy)ethylamine (**7**). Figure 8A shows the ^{1}H NMR spectrum of the monomer **8**. The peak at 6.30 ppm corresponds to the olefinic protons, and two doublet peaks at 1.36−1.39 and 1.47−1.51 ppm originate from the bridge-methylene protons of the *cis*-norbornene structure. Further-

dx.doi.org/10.1021/om5006897 | *Organometallics* 2014, 33, 4323−4335

more, the protons of the methyl group of the side chain are found at 3.37 ppm.

The block copolymers **10** were synthesized by chain extension of monomer **8** to the second amidoferrocenyl-containing monomer **5** via a one-pot two-step sequential ROMP. The preparation of the first block, polymer **9**, was accomplished with nearly 100% monomer conversion in 8 min, which was demonstrated by the disappearance of the peak at 6.30 ppm corresponding to the olefinic protons of monomer **8** and the appearance of new two broad peaks at 5.51 and 5.75 ppm corresponding to the olefinic protons of polymers (Figure 8B). The SEC results (Figures S32−S34, Supporting Information) show the good monodispersity (PDI < 1.1) of polymers **9** and demonstrate the controlled polymerization of monomer **8**. Full characterization of polymers **9** is detailed in the Supporting Information. Figure 8C shows the ^{1}H NMR spectrum of the block copolymer **10**. The protons of the Cp of the ferrocenyl groups are located at 4.71, 4.32, and 4.19 ppm, respectively. The peak at 6.47 ppm corresponds to the proton of the amido group in the amidoferrocenyl block. The presence of the above new peaks indicates the successful preparation of the block copolymers **10**.

Similarly, a series of amidoferrocenyl-containing copolymers **10** were synthesized with various molar feed ratios of monomer **8** and **5** to catalyst **1**. The polymerization of monomer **8** is finished at nearly 100% conversion within 8 min, even when the molar feed ratio of monomer **8** to **1** was increased to 200:1. However, for the second block, reaction times longer than 60 min (48 h in this study) were necessary when the feed ratio of monomer **5** to **1** was increased to 100:1. The most obvious difference in structure between monomers **5** and **8** is the presence of the amidoferrocenyl moiety in **5**. Thus, it is believed that the polymerization is slowed down by the presence of the amidoferrocenyl moiety due to steric constraint of the linked ferrocenyl bulk.[95] Furthermore, the block copolymers **10** show a better solubility than the homopolymers **6**. All of the prepared copolymers are soluble in DCM, $CHCl_3$, THF, DMF, and DMSO, and the small copolymers are even soluble in acetone, acetonitrile, and ethyl acetate.

3.5. Molecular Weight Analysis of Block Copolymers 10. The MWs of polymers **9** and block copolymers **10** were characterized by end-group analysis, MALDI-TOF MS, and SEC, respectively. The polymerization degrees of the first, polymers **9**, were first obtained by end-group analysis using the ^{1}H NMR spectra of polymers **9** in CD_3CN (Figure S27, Supporting Information). Then, the polymerization degrees of the second block, polymers **10**, were calculated by comparing the integration of the methyl proton (3.355 ppm) with that of the protons of the amido group (6.472 ppm) and Cp rings (4.710, 4.318, and 4.189 ppm), respectively. As shown in Table 3, the polymerization degrees from end-group analysis (n_{p2}) are very close to that obtained using the ^{1}H NMR conversion (n_{p1}). The number of amidoferrocenyl units in the copolymers **10** was also determined using the Bard−Anson electrochemical method. The estimated values of electrons (n_{p3}) for all of the copolymers showed a good consistency with the value of n_{p1}, as well. As shown in Figure 9, the MALDI-TOF MS of the small copolymer $\mathbf{10}^{6/3}$, in which the molar feed ratio of monomer **8** and **5** to **1** is 6:3:1, shows well-defined individual peaks for polymer fragments that are separated by 550 Da (MW of monomer **5**) and 309 Da (MW of monomer **8**), respectively. The MW found for $(C_6H_6)(C_{16}H_{23}NO_5)_6(C_{28}H_{34}N_2O_6Fe)_3(C_2H_2)Na$ is 3633.9 Da, which is very close to the calculated value of 3633.4 Da. For polymers **9**, the MW from SEC analysis (Figures S32−S34, Supporting Information) is also close to the theoretical values obtained by ^{1}H NMR conversion. For the corresponding copolymers **10**, as for the homopolymers **6**, the MWs obtained by SEC are always smaller than the calculated values. Fortunately, the PDI values for all the copolymers **10** are less than 1.15, which shows the good monodispersity of the copolymers.

3.6. Redox Properties and Electrochemical Sensing of ATP^{2-} for the Block Copolymers 10. The side chain amidoferrocenyl containing block copolymers **10** were studied by CV using $[FeCp^*_2]$ as the internal reference. The CVs were recorded in DCM (Figure 10 and Figures S44−S46 (Supporting Information)), and the $E_{1/2}$ data (measured vs $[FeCp^*_2]$) are gathered in Table S3 (Supporting Information). As shown in Figure 10A, a single oxidation wave is observed for the ferrocenyl groups of the copolymer $\mathbf{10}^{100/50}$, and this single wave shows better reversibility and less adsorption than that of **6**, which is taken into account by the solubilizing property of the TEG chains in **10**. Some adsorption is still observable, however, as characterized by an intensity ratio i_a/i_c (0.9) that is lower than 1 and a ΔE value that is lower (0.020 V) that the Nernstian value of 0.059 V at 25 °C. The anodic and cathodic CV waves are also slightly broader than those of the monomer **5**, which is probably due to the nonequivalence of all the ferrocenyl groups in the polymer chain. The $Fe^{III/II}$ oxidation potential of the ferrocenyl redox center is found around 680 mV as well.

The accessibility of modified electrodes[85−90] has also been explored. Indeed, upon scanning around the oxidation potential of the amidoferrocenyl group, the copolymers are adsorbed onto electrodes (see Figure S46B). Thus, modification of electrodes using the copolymers **10** has been successful. Figure 10B and Figure S46C show the electrochemical behavior of modified electrodes in DCM containing only the supporting electrolyte. A well-defined symmetrical redox wave that is characteristic of a surface-confined redox couple is observed, including the expected linear relationship of peak current with potential sweep rate. Furthermore, repeated scanning does not change the CVs, which indicates that the modified electrode is stable. There is no structural change during the electrochemical redox process, as no splitting between the oxidation and reduction peaks is observed (ΔE = 0 mV).

Finally, electrochemical recognition of $[n\text{-}Bu_4N]_2[ATP]$ by the copolymer **10** was also found to be possible. As shown in Figure 11, the addition of $[n\text{-}Bu_4N]_2[ATP]$ to an electrochemical cell containing the Pt electrode modified with copolymer $\mathbf{10}^{100/50}$ in DCM provoked the appearance of a new wave at a potential less positive than the initial wave. The intensity of the initial wave decreased, while that of the new wave increased. The difference in amidoferrocenyl redox potential between the initial wave and the new wave (ΔE) is 150 mV: i.e., 20 mV larger than that obtained using the modified Pt electrode with polymer $\mathbf{6}^{50}$. This might possibly be the consequence of encapsulation by the triethylene glycol branch network of the amidoferrocene−ATP interaction. Consequently for the qualitative recognition of ATP^{2-} anions the Pt electrode modified with the copolymer **10** shows a better effect in comparison to that modified with the homopolymer **6**.

dx.doi.org/10.1021/om5006897 | Organometallics 2014, 33, 4323−4335

4. CONCLUSION

These series of side chain amidoferrocenyl containing homopolymers and block copolymers that were successfully synthesized by controlled and living ROMP catalyzed by Grubbs' third-generation catalyst (**1**) are monodisperse and can reach up to 332 units, with the solubility decreasing as the number of monomer units increases. Given the relatively good solubility of up to large sizes, they could be easily used. They very efficiently modified Pt electrodes with excellent stability and robustness, and the modified Pt electrodes recognized ATP^{2-} anions. The Pt electrodes modified with block copolymers show a slightly better qualitative sensing of ATP^{2-} anion in comparison to those modified with the corresponding homopolymers, possibly because the triethylene glycol branch network favors the amidoferrocene−ATP interaction by encapsulation. Quantitative recognition (titration) of ATP^{2-} is obtained, with the DCM solutions of the homopolymers showing the interaction of two amidoferrocenyl groups with each ATP^{2-}. This leads us to conclude that a chelating intramolecular H bond occurs with the β and γ phosphate groups of ATP^{2-} and a single H bond between the α phosphate and another amidoferrocenyl group involves intermolecular H bonding: i.e., a polymeric network of H bonds.

■ ASSOCIATED CONTENT

Ⓢ Supporting Information

Text, figures, and tables giving general data, including solvents, apparatuses, reagents, syntheses of intermediates, ^{1}H, ^{13}C, and DOSY NMR, IR, and MALDI-TOF mass spectra, cyclic voltammograms, and SEC of the polymers. This material is available free of charge via the Internet at http://pubs.acs.org.

■ AUTHOR INFORMATION

Present Address

[§]On sabbatical leave from the Key Laboratory of Leather Chemistry and Engineering of Ministry of Education, Sichuan University, Chengdu 610065, People's Republic of China.

Notes

The authors declare no competing financial interest.

■ ACKNOWLEDGMENTS

Financial support from the National Science Foundation of China (21106088), the Ph.D. Program Foundation of the Ministry of Education of China (20110181120079), the University of Bordeaux, the Centre National de la Recherche Scientifique, and L'Oréal are gratefully acknowledged.

■ REFERENCES

(1) Abd-El-Aziz, A. S.; Manners, I. *Frontiers in Transition-Metal-Containing Polymers*; Wiley: Hoboken, NJ, 2007.
(2) Manners, I. *Science* **2001**, *294*, 1664−1666.
(3) Wang, X.; Guerin, G.; Wang, H.; Wang, Y.; Manners, I.; Winnik, M. A. *Science* **2007**, *317*, 644−647.
(4) Abd-El-Aziz, A. S. *Coord. Chem. Rev.* **2002**, *233*−*234*, 177−191.
(5) Jakle, F. *Chem. Rev.* **2010**, *110*, 3985−4022.
(6) Whittell, G. R.; Hager, M. D.; Schubert, U. S.; Manners, I. *Nat. Mater.* **2011**, *10*, 176−188.
(7) Qiu, H.; Cambridge, G.; Winnik, M. A.; Manners, I. *J. Am. Chem. Soc.* **2013**, *135*, 12180−12183.
(8) Qiu, H.; Du, V. A.; Winnik, M. A.; Manners, I. *J. Am. Chem. Soc.* **2013**, *135*, 17739−17742.
(9) McGrath, N.; Schacher, F. H.; Qiu, H.; Mann, S.; Winnik, M. A.; Manners, I. *Polym. Chem.* **2014**, *5*, 1923−1929.
(10) Burnworth, M.; Tang, L.; Kumpfer, J. R.; Duncan, A. J.; Beyer, F. L.; Fiore, G. L.; Rowan, S. J.; Weder, C. *Nature* **2011**, *472*, 334−337.
(11) Holliday, B. J.; Swager, T. M. *Chem. Commun.* **2005**, 23−36.
(12) Hardy, C. G.; Ren, L.; Zhang, J.; Tang, C. *Isr. J. Chem.* **2012**, *52*, 230−245.
(13) Hardy, C. G.; Ren, L.; Tamboue, T. C.; Tang, C. *J. Polym. Sci., Part A* **2011**, *49*, 1409−1420.
(14) Astruc, D. *Nat. Chem.* **2012**, *4*, 255−267.
(15) Ornelas, C.; Ruiz, J.; Belin, C.; Astruc, D. *J. Am. Chem. Soc.* **2009**, *131*, 590−601.
(16) Duan, Q.; Cao, Y.; Li, Y.; Hu, X.; Xiao, T.; Lin, C.; Pan, Y.; Wang, L. *J. Am. Chem. Soc.* **2013**, *135*, 10542−10549.
(17) Feng, C.; Lu, G.; Li, Y.; Huang, X. *Langmuir* **2013**, *29*, 10922−10931.
(18) Dong, Z.; Cao, Y.; Yuan, Q.; Wang, Y.; Li, J.; Li, B.; Zhang, S. *Macromol. Rapid Commun.* **2013**, *34*, 867−872.
(19) Yan, Q.; Yuan, J.; Cai, Z.; Xin, Y.; Kang, Y.; Yin, Y. *J. Am. Chem. Soc.* **2010**, *132*, 9268−9270.
(20) Tonhauser, C.; Alkan, A.; Schömer, M.; Dingels, C.; Ritz, S.; Mailänder, V.; Frey, H.; Wurm, F. R. *Macromolecules* **2013**, *46*, 647−655.
(21) Elbert, J.; Gallei, M.; Rüttiger, C.; Brunsen, A.; Didzoleit, H.; Stühn, B.; Rehahn, M. *Organometallics* **2013**, *32*, 5873−5878.
(22) Nakahata, M.; Takashima, Y.; Yamaguchi, H.; Harada, A. *Nat. Commun.* **2011**, *2*, No. 511, DOI: 10.1038/ncomms1521.
(23) Xia, W.; Hu, X.; Chen, Y.; Lin, C.; Wang, L. *Chem. Commun.* **2013**, *49*, 5085−5087.
(24) Rider, D. A.; Manners, I. *Polym. Rev.* **2007**, *47*, 165−195.
(25) Kaifer, A. E. *Eur. J. Inorg. Chem.* **2007**, 5015−5027.
(26) Daniel, M. C.; Ruiz, J.; Astruc, D. *J. Am. Chem. Soc.* **2003**, *125*, 1150−1151.
(27) Ornelas, C.; Méry, D.; Cloutet, E.; Ruiz, J.; Astruc, D. *J. Am. Chem. Soc.* **2008**, *130*, 1495−1506.
(28) Eloi, J. C.; Chabanne, L.; Whittell, G. R.; Manners, I. *Mater. Today* **2008**, *11*, 28−36.
(29) (a) Nguyen, P.; Gómez-Elipe, P.; Manners, I. *Chem. Rev.* **1999**, *99*, 1515−1548. (b) Ahmed, R.; Patra, S. K.; Hamley, I. W.; Manners, I.; Faul, C. F. J. *J. Am. Chem. Soc.* **2013**, *135*, 2455−2458. (c) Deraedt, C.; Rapakousiou, A.; Wang, Y.; Salmon, L.; Bousquet, M.; Astruc, D. *Angew. Chem., Int. Ed.* **2014**, DOI: 10.1002/chem.201403085.
(30) Pittman, C. U.; Lai, J. C.; Vanderpool, D. P.; Good, M.; Prado, R. *Macromolecules* **1970**, *3*, 746−754.
(31) Pittman, C. U.; Voges, R. L.; Jones, W. B. *Macromolecules* **1971**, *4*, 298−302.
(32) Pittman, C. U.; Voges, R. L.; Jones, W. B. *Macromolecules* **1971**, *4*, 291−297.
(33) Pittman, C. U.; Ayers, O. E.; McManus, S. P.; Sheats, J. E.; Whitten, C. E. *Macromolecules* **1971**, *4*, 360−362.
(34) Pittman, C. U.; Hirao, A. *J. Polym. Sci., Polym. Chem.* **1977**, *15*, 1677−1686.
(35) Pittman, C. U.; Hirao, A. *J. Polym. Sci., Polym. Chem.* **1978**, *16*, 1197−1209.
(36) Pittman, C. U.; Lin, C. C. *J. Polym. Sci., Polym. Chem.* **1979**, *17*, 271−275.
(37) Wright, M. E. *Organometallics* **1990**, *9*, 853−856.
(38) Deschenaux, R.; Izvolensk, V.; Turpin, F.; Guillon, D.; Heinrich, B. *Chem. Commun.* **1996**, 439−440.
(39) Hadjichristidis, N.; Pitsikalis, M.; Pispas, S.; Iatrou, H. *Chem. Rev.* **2001**, *101*, 3747−3792.
(40) Buchmeiser, M. R. *Chem. Rev.* **2000**, *100*, 1565−1604.
(41) Matyjaszewski, K.; Xia, J. *Chem. Rev.* **2001**, *101*, 2921−2990.
(42) Kamigaito, M.; Ando, T.; Sawamoto, M. *Chem. Rev.* **2001**, *101*, 3689−3745.
(43) Wang, J.-S.; Matyjaszewski, K. *J. Am. Chem. Soc.* **1995**, *117*, 5614−5615.
(44) Percec, V.; Barboiu, B. *Macromolecules* **1995**, *28*, 7970−7972.

(45) Kato, M.; Kamigaito, M.; Sawamoto, M.; Higashihara, T. *Macromolecules* **1995**, *28*, 1721−1723.
(46) Zhang, J.; Ren, L.; Hardy, C. G.; Tang, C. *Macromolecules* **2012**, *45*, 6857−6863.
(47) Hawker, C. J.; Bosman, A. W.; Harth, E. *Chem. Rev.* **2001**, *101*, 3661−3688.
(48) (a) Bielawskia, C. W.; Grubbs, R. H. *Prog. Polym. Sci.* **2007**, *32*, 1−29. (b) Grubbs, R. H. Living ring-opening olefin metathesis polymerization. In *Polymer Science: A Comprehensive Reference*; Elsevier: Amsterdam, 2012; Vol. *4*, pp 21−29. (c) Deraedt, C.; d'Halluin, M.; Astruc, D. *Eur. J. Inorg. Chem.* **2013**, 4881−4908. (d) Knall, A.-C.; Slugovc, C. In *Olefin Metathesis. Theory and Practice*; Grela, K., Ed.; Wiley: Hoboken, NJ, 2014; pp 269−284.
(49) Albagli, D.; Bazan, G. C.; Wrighton, M. S.; Schrock, R. R. *J. Am. Chem. Soc.* **1992**, *114*, 4150−4158.
(50) Albagli, D.; Bazan, G. C.; Schrock, R. R.; Wrighton, M. S. *J. Phys. Chem.* **1993**, *97*, 10211−10216.
(51) Albagli, D.; Bazan, G. C.; Schrock, R. R.; Wrighton, M. S. *J. Am. Chem. Soc.* **1993**, *115*, 7328−7334.
(52) Watson, K. J.; Zhu, J.; Nguyen, S. T.; Mirkin, C. A. *J. Am. Chem. Soc.* **1999**, *121*, 462−463.
(53) Watson, K. J.; Zhu, J.; Nguyen, S. T.; Mirkin, C. A. *Pure Appl. Chem.* **2000**, *72*, 67−72.
(54) Watson, K. J.; Nguyen, S. T.; Mirkin, C. A. *J. Organomet. Chem.* **2000**, *606*, 79−83.
(55) Watson, K. J.; Park, S.; Im, J.; Nguyen, S. T.; Mirkin, C. A. *J. Am. Chem. Soc.* **2001**, *123*, 5592−5593.
(56) Liu, X.; Guo, S.; Mirkin, C. A. *Angew. Chem., Int. Ed.* **2003**, *42*, 4785−4789.
(57) Gibbs, J. M.; Park, S.; Anderson, D. R.; Watson, K. J.; Mirkin, C. A.; Nguyen, S. T. *J. Am. Chem. Soc.* **2005**, *127*, 1170−1178.
(58) Abd-El-Aziz, A. S.; Todd, E. K.; Ma, G. Z. *J. Polym. Sci., Part A* **2001**, *39*, 1216−1231.
(59) Abd-El-Aziz, A. S.; May, L. J.; Hurd, J. A.; Okasha, R. M. *J. Polym. Sci., Part A* **2001**, *39*, 2716−2722.
(60) Abd-El-Aziz, A. S. *Macromol. Rapid Commun.* **2002**, *23*, 995−1031.
(61) Abd-El-Aziz, A. S.; Todd, E. K.; Okasha, R. M.; Wood, T. E. *Macromol. Rapid Commun.* **2002**, *23*, 743−748.
(62) Abd-El-Aziz, A. S.; Okasha, R. M.; Afifi, T. H.; Todd, E. K. *Macromol. Chem. Phys.* **2003**, *204*, 555−563.
(63) Abd-El-Aziz, A. S.; Okasha, R. M.; Afifi, T. H. *J. Inorg. Organomet. Polym.* **2004**, *14*, 269−278.
(64) Abd-El-Aziz, A. S.; Todd, E. K.; Okasha, R. M.; Shipman, P. O.; Wood, T. E. *Macromolecules* **2005**, *38*, 9411−9419.
(65) Abd-El-Aziz, A. S.; Okasha, R. M.; May, L. J.; Hurd, J. *J. Polym. Sci., Part A* **2006**, *44*, 3053−3070.
(66) Abd-El-Aziz, A. S.; Winram, D. J.; Shipman, P. O.; Bichler, L. *Macromol. Rapid Commun.* **2010**, *31*, 1992−1997.
(67) Yang, H.; Lin, S.; Yang, H.; Lin, C.; Tsai, L.; Huang, S.; Chen, I. W.; Chen, C.; Jin, B.; Luh, T. *Angew. Chem., Int. Ed.* **2006**, *45*, 726−730.
(68) Yang, H.; Lin, S.; Liu, Y.; Wang, Y.; Chen, M.; Sheu, H.; Tsou, D.; Lin, C.; Luh, T. *J. Organomet. Chem.* **2006**, *691*, 3196−3200.
(69) Lin, C.; Yang, H.; Lin, N.; Hsu, I.; Wang, Y.; Luh, T. *Chem. Commun.* **2008**, 4484−4486.
(70) Luh, T.; Yang, H.; Lin, N.; Lin, S.; Lee, S.; Chen, C. *Pure Appl. Chem.* **2008**, *80*, 819−829.
(71) Yang, H.; Lee, S.; Chen, C.; Lin, N.; Yang, H.; Jina, B.; Luh, T. *Chem. Commun.* **2008**, 6158−6160.
(72) Lin, N.; Lee, S.; Yu, J.; Chen, C.; Huang, S.; Luh, T. *Macromolecules* **2009**, *42*, 6986−6991.
(73) Chou, C.; Lee, S.; Chen, C.; Biju, A. T.; Wang, H.; Wu, Y.; Zhang, G.; Yang, K.; Lim, T.; Huang, M.; Tsai, P.; Lin, K.; Huang, S.; Chen, C.; Luh, T. *J. Am. Chem. Soc.* **2009**, *131*, 12579−12585.
(74) Luh, T. *Acc. Chem. Res.* **2013**, *46*, 378−389.
(75) Zhu, L.; Flook, M. M.; Lee, S.; Chan, L.; Huang, S.; Chiu, C.; Chen, C.; Schrock, R. R.; Luh, T. *Macromolecules* **2012**, *45*, 8166−8171.
(76) Yeh, N.; Chen, C.; Lee, S.; Wu, H.; Chen, C.; Luh, T. *Macromolecules* **2012**, *45*, 2662−2667.
(77) Dragutan, I.; Dragutan, V.; Fischer, H. *J. Inorg. Organomet. Polym.* **2008**, *18*, 311−324.
(78) Zha, Y.; Thaker, H. D.; Maddikeri, R. R.; Gido, S. P.; Tuominen, M. T.; Tew, G. N. *J. Am. Chem. Soc.* **2012**, *134*, 14534−14541.
(79) Sanford, M. S.; Love, J. A.; Grubbs, R. H. *Organometallics* **2001**, *20*, 5314−5318.
(80) Camm, K. D.; Castro, N. M.; Liu, Y.; Czechura, P.; Snelgrove, J. L.; Fogg, D. E. *J. Am. Chem. Soc.* **2007**, *129*, 4168−4169.
(81) Boisselier, E.; Diallo, A. K.; Salmon, L.; Ornelas, C.; Ruiz, J.; Astruc, D. *J. Am. Chem. Soc.* **2010**, *132*, 2729−2742.
(82) Llevot, A.; Astruc, D. *Chem. Soc. Rev.* **2012**, *41*, 242−257.
(83) Iyer, A. K.; Khaled, G.; Fang, J.; Maeda, H. *Drug Discovery Today* **2006**, *11*, 813−818.
(84) Flanagan, J. B.; Margel, S.; Bard, A. J.; Anson, F. C. *J. Am. Chem. Soc.* **1978**, *100*, 4248−4253.
(85) Murray, R. W. *Electroanal. Chem.* **1984**, *13*, 191−368.
(86) Li, W.; Chung, H.; Daeffler, C.; Johnson, J. A.; Grubbs, R. H. *Macromolecules* **2012**, *45*, 9595−9603.
(87) Abruña, H. D. *Coord. Chem. Rev.* **1988**, *86*, 135−189.
(88) Bard, A. J.; Faulkner, L. R. *Electrochemical Methods: Fundamentals and Applications*, 2nd ed.; Wiley: New York, 2001.
(89) Zanello, P. *Inorganic Electrochemistry. Theory, Practice and Application*; RSC Publishing: Cambridge, U.K., 2003.
(90) (a) Ruiz, J.; Astruc, D. *C. R. Acad. Sci., Ser. IIc: Chim.* **1998**, *1*, 21−27. (b) Geiger, W. E. *Organometallics* **2007**, *26*, 5738−5765.
(91) Beer, P. D. *Acc. Chem. Res.* **1998**, *31*, 71−80.
(92) Beer, P. D.; Gale, P. A. *Angew. Chem., Int. Ed.* **2001**, *40*, 486−516.
(93) Astruc, D.; Daniel, M.-C.; Ruiz, J. *Chem. Commun.* **2004**, 2637−2649.
(94) Schinle, F.; Crider, P. E.; Vonderach, M.; Weis, P.; Hampe, O.; Kappes, M. M. *Phys. Chem. Chem. Phys.* **2013**, *15*, 6640−50.
(95) For a kinetic approach to ROMP synthesis of precision functional poly(norbornene) polymers, see: Moatsou, D.; Hansell, C. F.; O'Reilly, R. K. *Chem. Sci.* **2014**, *5*, 2246−2250.